Title

A novel artificial condensed matter lattice and a new platform for one-dimensional topological phases

Journal

Science Advances, 3(3)

ISSN

2375-2548

Authors

Belopolski, Ilya

Xu, Su-Yang

Koirala, Nikesh

et al.

Publication Date

2017-03-03

DOI

10.1126/sciadv.1501692

Peer reviewed

PHYSICAL SCIENCE

A novel artificial condensed matter lattice and a new platform for one-dimensional topological phases

Ilya Belopolski,[1]* Su-Yang Xu,[1] Nikesh Koirala,[2] Chang Liu,[3] Guang Bian,[1] Vladimir N. Strocov,[4] Guoqing Chang,[5] Madhab Neupane,[6] Nasser Alidoust,[1] Daniel Sanchez,[1] Hao Zheng,[1] Matthew Brahlek,[2] Victor Rogalev,[4,7] Timur Kim,[8] Nicholas C. Plumb,[4] Chaoyu Chen,[9] François Bertran,[9] Patrick Le Fèvre,[9] Amina Taleb-Ibrahimi,[9] Maria-Carmen Asensio,[9] Ming Shi,[4] Hsin Lin,[5] Moritz Hoesch,[8] Seongshik Oh,[2] M. Zahid Hasan[1,10,11]*

Engineered lattices in condensed matter physics, such as cold-atom optical lattices or photonic crystals, can have properties that are fundamentally different from those of naturally occurring electronic crystals. We report a novel type of artificial quantum matter lattice. Our lattice is a multilayer heterostructure built from alternating thin films of topological and trivial insulators. Each interface within the heterostructure hosts a set of topologically protected interface states, and by making the layers sufficiently thin, we demonstrate for the first time a hybridization of interface states across layers. In this way, our heterostructure forms an emergent atomic chain, where the interfaces act as lattice sites and the interface states act as atomic orbitals, as seen from our measurements by angle-resolved photoemission spectroscopy. By changing the composition of the heterostructure, we can directly control hopping between lattice sites. We realize a topological and a trivial phase in our superlattice band structure. We argue that the superlattice may be characterized in a significant way by a one-dimensional topological invariant, closely related to the invariant of the Su-Schrieffer-Heeger model. Our topological insulator heterostructure demonstrates a novel experimental platform where we can engineer band structures by directly controlling how electrons hop between lattice sites.

INTRODUCTION

While crystals found in nature offer a great richness of phenomena, recent progress in physics has also been driven by the study of engineered systems, where key material parameters or Hamiltonian matrix elements can be directly controlled in experiments to give rise to novel emergent properties. For example, the Haldane model for a Chern insulator was recently realized in an optical lattice of ultracold atoms (*1*), and a Weyl semimetal was observed in a photonic crystal with a double-gyroid lattice structure (*2*). Each advance required engineering a specific ultracold-atom optical lattice or photonic crystal. In both cases, these engineered lattices gave rise to an emergent band structure, analogous to the band structure formed by electrons in a crystal lattice, but with distinct properties and highly tuned parameters that gave rise to a novel phase of matter.

Here, we demonstrate an emergent band structure in a novel type of condensed matter lattice based on topological insulators (*3*, *4*). Specifically, we stack together layers of topological and trivial insulators to create a one-dimensional topological insulator heterostructure. Each interface in the heterostructure hosts a set of topologically protected interface states that hybridize with each other across the layers, giving rise to a superlattice band structure where the interfaces play the role of lattice sites, the topological surface states play the role of atomic orbitals, and the heterostructure acts as a one-dimensional atomic chain. Such a superlattice band structure is emergent in the sense that it arises only when many layers are stacked together, in the same way that an ordinary band structure arises as an emergent property of a crystal lattice. A similar heterostructure has previously been proposed as a simple theoretical model for a Weyl semimetal (*5*). Here, we experimentally realize and directly observe the first superlattice band structure of this type. We use molecular beam epitaxy to build the topological insulator heterostructure, and we use angle-resolved photoemission spectroscopy (ARPES) to study its band structure. By adjusting the pattern of layers in the heterostructure, we realize both a topological and a trivial phase, demonstrating that we can tune our system through a topological phase transition. Our work may lead to the realization of novel three-dimensional and one-dimensional symmetry-protected topological phases. Moreover, our topological insulator heterostructure provides a highly tunable emergent band structure in a true electron system, relevant for transport experiments and device applications.

We first provide a more detailed introduction to the topological insulator heterostructure and argue that our system forms a novel type of condensed matter lattice. A topological insulator heterostructure is built up of alternating layers of topologically trivial and nontrivial insulators. Here, we use Bi_2Se_3 as the topological insulator and $In_xBi_{2-x}Se_3$ as the trivial insulator (see Fig. 1A). We note that heterostructures of Bi_2Se_3 and In_2Se_3 have already been successfully synthesized (*6*–*8*). Bulk Bi_2Se_3 has a nontrivial $\mathbb{Z}_2$ invariant, $\nu_0 = 1$ (*9*, *10*). Under doping by In, bulk Bi_2Se_3 undergoes a topological phase transition to a topologically trivial phase with $\mathbb{Z}_2$ invariant, $\nu_0 = 0$ (*11*). In all samples considered here, all $In_xBi_{2-x}Se_3$ layers are well into the trivial phase. As a result, the topological invariant flips back and forth from layer to layer in the heterostructure, so that each interface hosts a set of topological interface states (*3*, *4*, *12*–*15*). Next, we note that these interface states have a finite penetration depth into the bulk of the crystal, so that for sufficiently thin

[1]Laboratory for Topological Quantum Matter and Spectroscopy (B7), Department of Physics, Princeton University, Princeton, NJ 08544, USA. [2]Department of Physics and Astronomy, Rutgers, The State University of New Jersey, Piscataway, NJ 08854 USA. [3]Department of Physics, South University of Science and Technology of China, Shenzhen, Guangdong 518055, China. [4]Swiss Light Source, Paul Scherrer Institut, CH-5232 Villigen PSI, Switzerland. [5]Department of Physics, National University of Singapore, Singapore 117542, Singapore. [6]Department of Physics, University of Central Florida, Orlando, FL 32816, USA. [7]Physikalisches Institut and Röntgen Center for Complex Material Systems, Universität Würzburg, 97074 Würzburg, Germany. [8]Diamond Light Source, Harwell Campus, Didcot OX11 0DE, UK. [9]Synchrotron SOLEIL, L'Orme des Merisiers, Saint-Aubin, BP 48, 91192 Gif-sur-Yvette, France. [10]Princeton Institute for the Science and Technology of Materials, Princeton University, Princeton, NJ 08544, USA. [11]Lawrence Berkeley National Laboratory, Berkeley, CA 94720, USA.
*Corresponding author. Email: ilyab@princeton.edu (I.B.); mzhasan@princeton.edu (M.Z.H.)

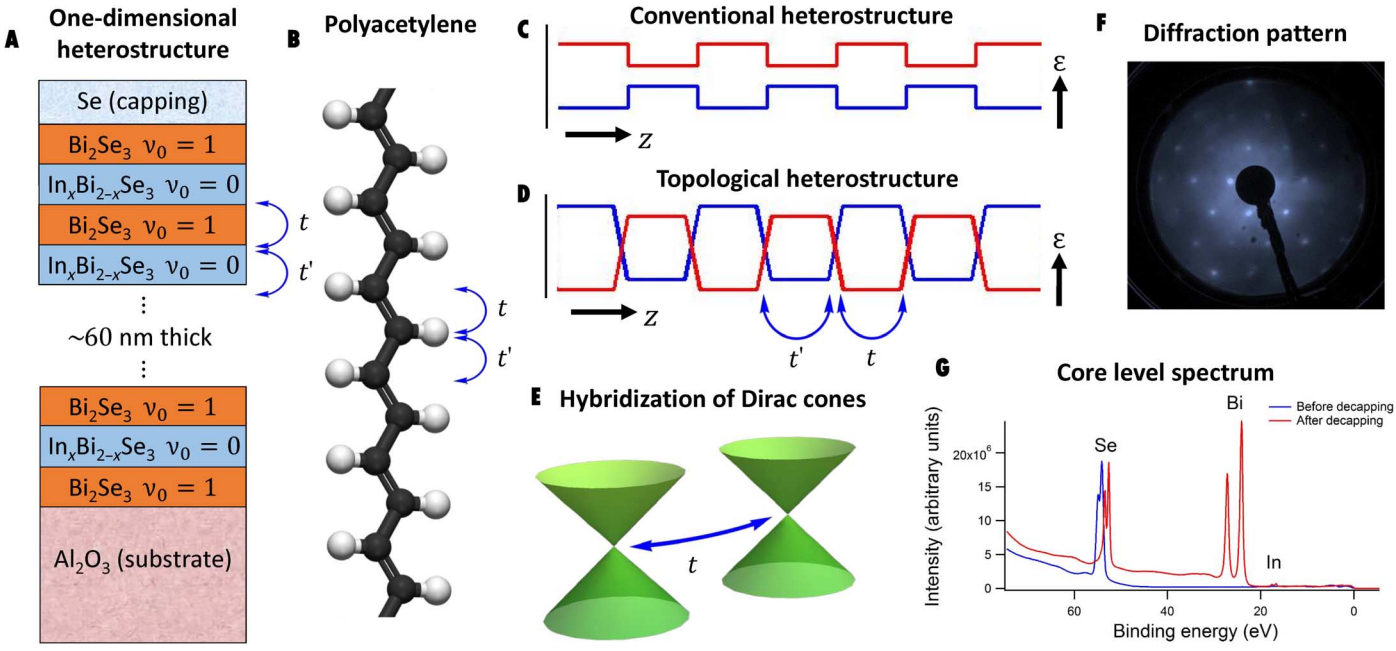

Fig. 1. Overview of the topological insulator heterostructure. (**A**) The heterostructure consists of a stack of alternating $\mathbb{Z}_2$ topological insulator layers and trivial insulator layers. We use Bi_2Se_3 as the topologically nontrivial layer and $In_xBi_{2-x}Se_3$ as the topologically trivial layer. The $\mathbb{Z}_2$ invariant is denoted by $\nu_0 = 1, 0$. An amorphous Se capping layer protects the sample in atmosphere and is removed by heating the sample in situ. (**B**) Our system realizes an emergent version of a polyacetylene chain, well known as a toy model in the study of one-dimensional topological phases. The model has two carbon atoms per unit cell, with one orbital each and with hopping amplitudes t and t' associated with the double and single carbon bonds. In the topological insulator heterostructure, the topological and trivial layers play the role of the double and single carbon bonds. (**C**) A conventional semiconductor heterostructure consists of an alternating pattern of materials with different band gaps. (**D**) In a topological insulator heterostructure, the band gaps in adjacent layers are inverted, giving rise to topologically protected Dirac cone interface states between layers. If the layers are thin, then adjacent Dirac cones may hybridize. This hybridization can be described by a hopping amplitude t across the topological layer and a hopping amplitude t' across the trivial layer. (**E**) Illustration of the Dirac cone surface states at each interface in the heterostructure, assuming no hybridization. With a hybridization t, the topological interface states form a superlattice band structure. A standard low-energy electron diffraction pattern (**F**) and a core-level photoemission spectrum (**G**) show that the samples are of high quality and that the Se capping layer was successfully removed by in situ heating, exposing a clean sample surface in vacuum.

layers, the topological interface states hybridize with each other across the layers and will be subject to an energy level repulsion (*16*, *17*). This hybridization can be captured by a hopping amplitude t across the topological layer and a hopping amplitude t' across the trivial layer. In this way, the topological insulator heterostructure can be viewed as an analog of a polyacetylene chain (Fig. 1B), where the topological insulator corresponds to the carbon double bond and the trivial insulator corresponds to the carbon single bond (or vice versa). Our heterostructure is similar to a conventional semiconductor heterostructure in that the band gap varies in z (Fig. 1C) (*18*, *19*). However, we see that new phenomena arise in a topological insulator heterostructure because the band gap inverts from layer to layer (Fig. 1D). Specifically, the hybridization of topological interface states, illustrated schematically in Fig. 1E, gives rise to a superlattice dispersion. In this way, the topological insulator heterostructure is a novel type of condensed matter lattice, where the interfaces correspond to the atomic sites and the topological insulator interface states correspond to the atomic orbitals. Because we can precisely control the thickness of the topological and trivial layers, this superlattice band structure is highly tunable. At the same time, it remains a true electron system, relevant for transport experiments and device applications. Further, if the Fermi level can be placed in the bulk band gap, then the underlying bulk bands of each heterostructure layer become irrelevant, and the transport properties are determined only by the superlattice band structure. This emergent band structure provides a new platform to realize novel phases in three dimensions, such as a magnetic Weyl semimetal (*5*). Further, we note that the energy level repulsion occurs between the electron states at the Dirac points, at $k_{\|} = 0$. As a result, the system can be well described as an atomic chain with a two-site basis and one orbital per site, leading to a two-band single-particle Hamiltonian. By implementing a chiral symmetry in the layer pattern of the heterostructure, it may be possible to realize a phase with strictly one-dimensional topological invariant protected by chiral symmetry, although further theoretical study may be necessary (see discussion below) (*20*–*22*). We note that before measurement by ARPES, we measure standard core-level spectra and diffraction patterns to confirm the high quality of our samples (see Fig. 1, F and G).

RESULTS

We next demonstrate that we have observed an emergent superlattice dispersion in our topological insulator heterostructure. We present a systematic study of four different $Bi_2Se_3/In_xBi_{2-x}Se_3$ superlattices: 4QL/4QL 20%, 4QL/2QL 25%, 4QL/2QL 15%, and 4QL/1QL 20% (see Fig. 2, A to D). In this notation, the first parameter refers to the thickness of the Bi_2Se_3 layer, the second parameter refers to the thickness of the $In_xBi_{2-x}Se_3$ layer; and the percentage refers to the In doping x of the $In_xBi_{2-x}Se_3$ layer. In Fig. 2 (E to H), we present the ARPES spectra of the four heterostructures along a cut through the $\bar{\Gamma}$ point, and in Fig. 2 (I to L), we present the same ARPES spectra with additional hand-drawn lines to mark the bands observed in the data. In Fig. 2 (M to P), we further present the energy distribution curves (EDCs) of photoemission intensity as a function of binding

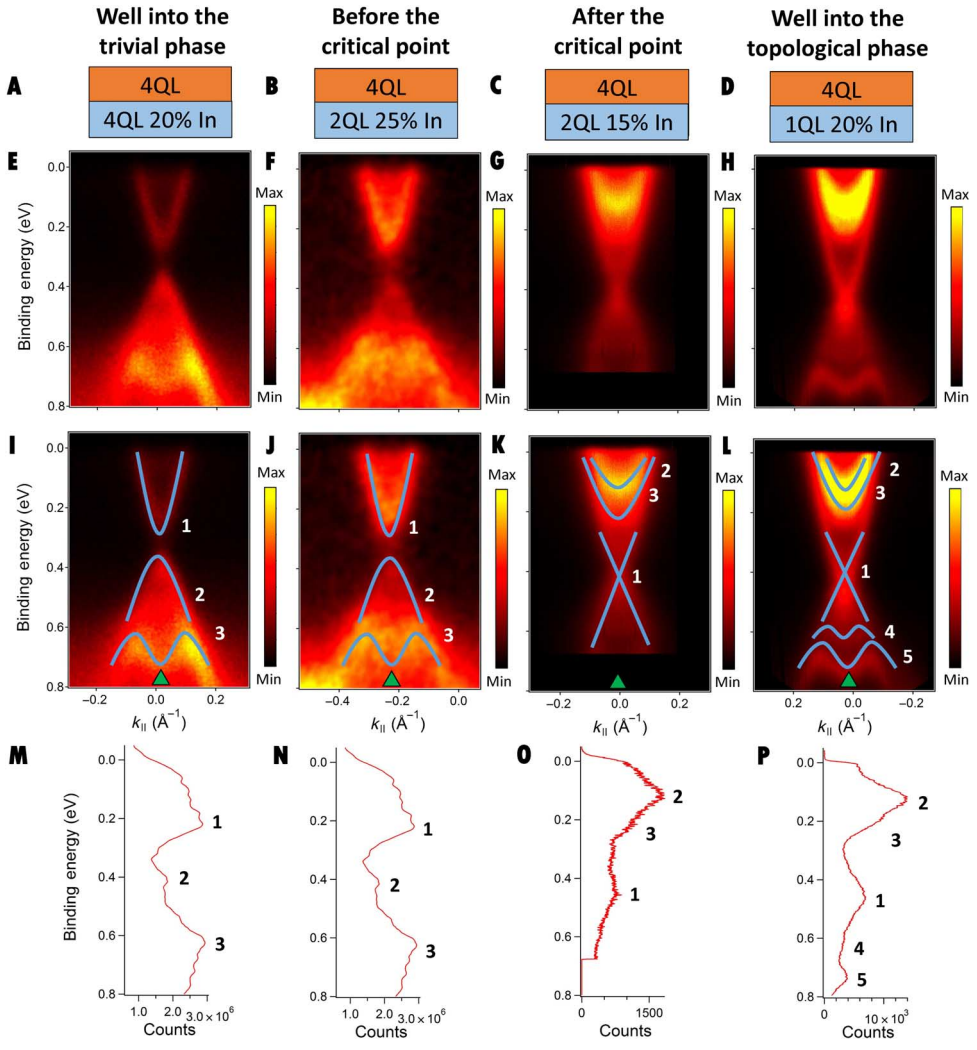

Fig. 2. Observation of an emergent superlattice band structure in trivial and topological phases. (**A** to **D**) The unit cells of the heterostructures studied, with different thicknesses and In doping of the $In_xBi_{2-x}Se_3$ layer. (**E** to **H**) ARPES spectra of the heterostructures. (E) and (F) show gapped surface states, whereas (G) and (H) show gapless surface states. Note that in all samples measured, the top layer of the superlattice, which is the only layer directly measured by ARPES, is 4QL of Bi_2Se_3. Nonetheless, the spectra differ markedly. (**I** to **L**) The same spectra as in (E) to (H), but with additional hand-drawn lines showing the key features of the spectra. In the 4QL/4QL 20% and 4QL/2QL 25% samples, we observe gapped topological surface states, 1 and 2, along with a valence band quantum well state, 3. By contrast, in 4QL/2QL 15% and 4QL/1QL 20%, we observe a gapless Dirac cone surface state, 1, and two conduction band quantum well states, 2 and 3, and in 4QL/1QL 20%, we observe two valence quantum well states, 4 and 5. We emphasize that the gapless Dirac cone is observed although the top Bi_2Se_3 layer is only 4QL thick. (**M** to **P**) EDCs through the $\bar{\Gamma}$ point of each spectrum in (E) to (H). The peaks corresponding to the bulk quantum well states and surface states are numbered on the basis of the correspondence with the full spectra (E to H).

energy at $k_{\parallel} = 0$. These curves correspond to a vertical line on the image plot, indicated by the green arrowheads in Fig. 2 (I to L). The gapless surface state, labeled 1 in 4QL/2QL 15% and 4QL/1QL 20%, is entirely inconsistent with a 4QL-thick film of Bi_2Se_3. It can only be explained by considering hybridization across the $In_xBi_{2-x}Se_3$ layer, demonstrating an emergent superlattice band structure arising from the hopping of Dirac cone interface states within the heterostructure. In addition, a gap opens from 4QL/2QL 15% to 4QL/2QL 25% without any observable bulk band inversion and without time-reversal symmetry breaking. This is an apparent contradiction with the basic theory of $\mathbb{Z}_2$ topological insulators. Again, this result demonstrates a superlattice dispersion. As we increase t/t', the top two lattice sites show larger hybridization, and a gap opens in the Dirac cone on the last site. Because ARPES is only sensitive to the top surface of the heterostructure, we can only observe the increased coupling to the top surface, and not the inversion of the superlattice bands. Our observation of (i) a gapless surface state on a 4QL-thick film of Bi_2Se_3 and (ii) a gap opening in a Bi_2Se_3 surface state without apparent band inversion demonstrates that we have observed a superlattice dispersion in our system. In this way, we have shown a novel type of electronic band structure, which arises from a lattice of topological insulator Dirac cones that are allowed to hybridize.

We provide a one-dimensional picture of the topological and trivial phases of the superlattice. We again consider 4QL/1QL 20%, as shown in Fig. 3 (A to D). Above, we argued that 4QL/1QL 20% has a gapless Dirac cone because $t < t'$. We note that the different hopping amplitude arises from the large bulk band gap and large thickness of the Bi_2Se_3 layer relative to the $In_xBi_{2-x}Se_3$ layer, as illustrated in Fig. 3E. Alternatively, we can consider how orbitals pair up and gap out in real space. We see that, in the topological phase, there are two end modes left without a pairing partner (see Fig. 3F). We contrast the topological

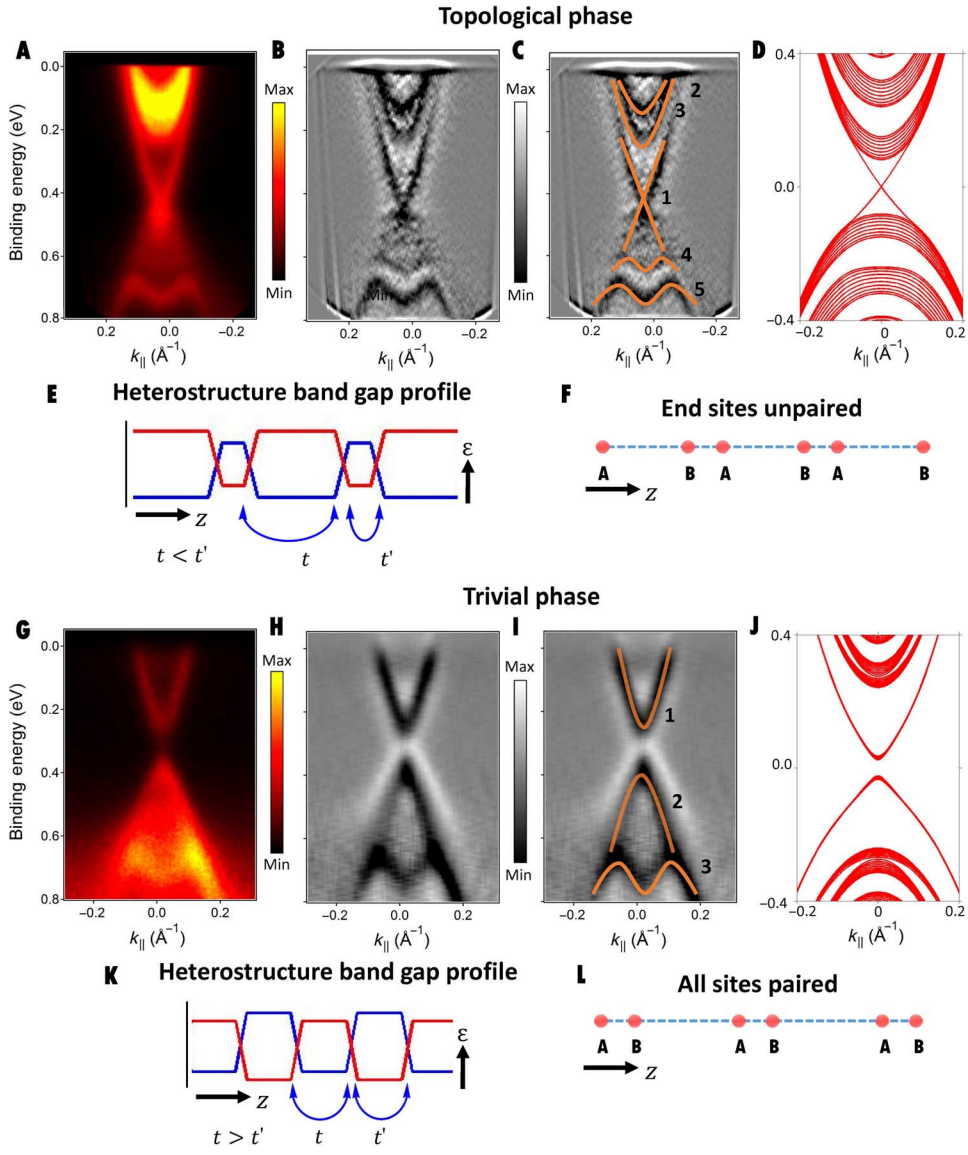

Fig. 3. Realization of the Su-Schrieffer-Heeger (SSH) model. ARPES spectrum of 4QL/1QL 20% (**A**), with a second-derivative map of the same spectrum (**B**) and the same second-derivative map (**C**) with additional hand-drawn lines highlighting the gapless surface state and the two quantum well states in the conduction and valence bands. (**D**) A tight-binding calculation demonstrating a topological phase qualitatively consistent with our experimental result. (**E**) A cartoon of the band gap profile of the 4QL/1QL 20% heterostructure. The trivial layer is much thinner than the topological layer; thus, $t < t'$, and we are in the SSH topological phase. (**F**) The SSH topological phase can be understood as a phase where the surface states pair up with their nearest neighbors and gap out but where the pairing takes place in such a way that there is an unpaired lattice site at the end of the atomic chain. ARPES spectrum of 4QL/4QL 20% (**G**), with a second-derivative map of the same spectrum (**H**) and the same second-derivative map (**I**) with additional hand-drawn lines highlighting the gapped surface state and the quantum well state in the valence band. (**J**) A tight-binding calculation demonstrating a trivial phase qualitatively consistent with our experimental result. (**K**) A cartoon of the band gap profile of the 4QL/4QL 20% heterostructure. The trivial layer is as thick as the topological layer, with a larger band gap due to high In doping; thus, $t > t'$, and we are in the SSH trivial phase. (**L**) The SSH trivial phase can be understood as a phase where all lattice sites in the atomic chain have a pairing partner.

phase with the trivial phase observed in 4QL/4QL 20%, as shown in Fig. 3 (G to J). In this case, $t > t'$, because the trivial phase has a larger band gap than the topological phase, as illustrated in Fig. 3K. Alternatively, the real space pairing leaves no lattice site without a pairing partner (see Fig. 3L). We see that our observation of a topological and trivial phase in a topological insulator heterostructure can be understood in terms of an emergent one-dimensional atomic chain where the termination of the chain is either on a strong or on a weak bond.

We present the ARPES spectra of other compositions in the topological and trivial phase to provide a systematic check of our results. First, we compare 4QL/1QL 10% and 4QL/1QL 15% with 4QL/1QL 20%. The unit cells of these lattices are illustrated in Fig. 4 (A to C). The ARPES spectra are shown in Fig. 4 (D to F). We also show an EDC at $k_{||} = 0$ in Fig. 4 (G to I), as indicated by the green arrowheads in Fig. 4 (D to F). We find that 4QL/1QL 10% and 4QL/1QL 15% also host a gapless surface state and are also topological. This is expected because we have further decreased the In concentration in the trivial layer, increasing the hybridization t and pushing the sample further into the topological phase. Next, we compare 3QL/3QL 20% with 4QL/4QL 20%. The unit cells are illustrated in Fig. 4 (J to L). The ARPES spectra

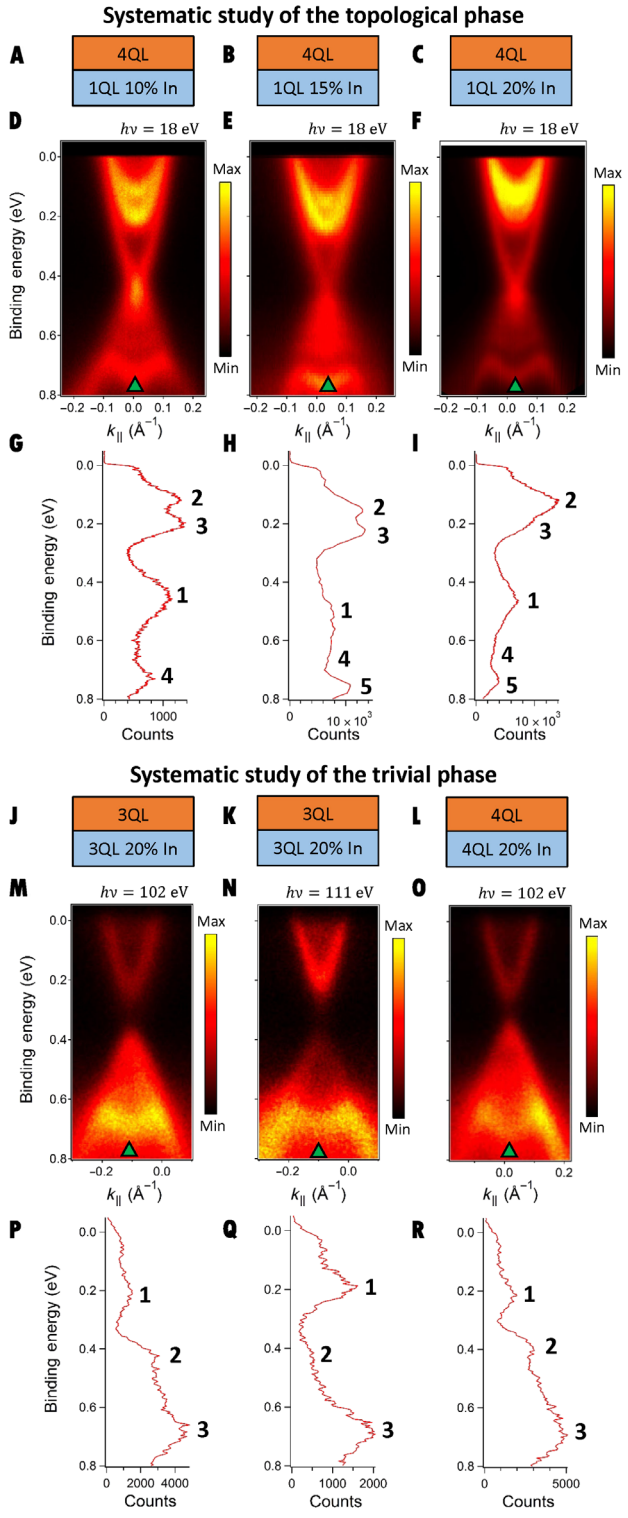

Fig. 4. Systematic study of the topological and trivial phases. (**A** to **F**) ARPES spectra of the 4QL/1QL samples at $h\nu$ = 18 eV with varying concentrations of In, showing a robust topological phase. (**G** to **I**) EDCs through the $\bar{\Gamma}$ point of each spectrum in (A) to (C). (**J** to **O**) ARPES spectra of the 3QL/3QL 20% and 4QL/4QL 20% samples at $h\nu$ = 102 eV and of the 3QL/3QL 20% sample at $h\nu$ = 111 eV, showing a robust trivial phase. (**P** to **R**) EDCs through the $\bar{\Gamma}$ point of each spectrum in (G) to (I).

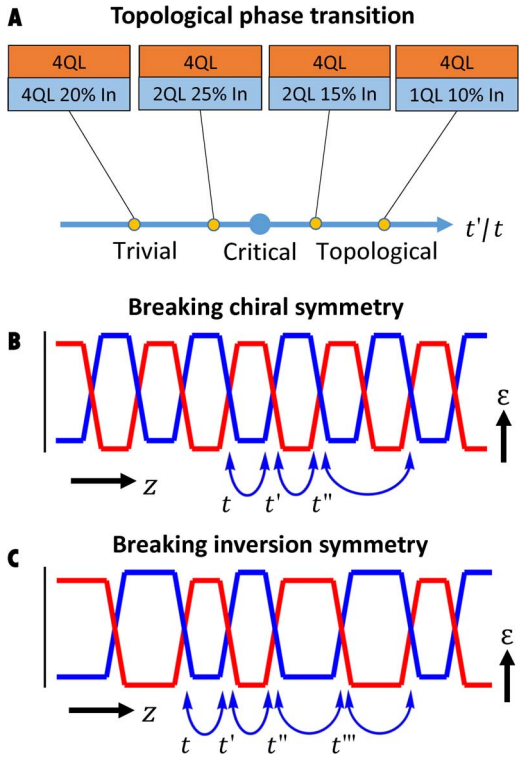

Fig. 5. Phase diagram of a tunable emergent superlattice band structure. (**A**) By varying the hopping t' across the trivial layer, we realize a trivial phase and a topological phase in our superlattice band structure. (**B**) In the heterostructures demonstrated here, we expect that only nearest-neighbor hopping is relevant, giving rise to an emergent chiral symmetry along the stacking direction. By using thinner layers, we propose to introduce a next nearest-neighbor hopping, breaking this chiral symmetry. This may change the topological classification of our system. (**C**) By doubling the unit cell, we can break inversion symmetry. This will give rise to a spinful superlattice dispersion.

are shown in Fig. 4 (M to O), and an EDC at $k_{||} = 0$ is shown in Fig. 4 (P to R). We find that 3QL/3QL 20% is also in the trivial phase, with a gap in the surface states larger than that in 4QL/4QL 20%. This is consistent with earlier ARPES studies of single thin films of Bi_2Se_3 on a topologically trivial substrate (*16*, *17*). For 3QL/3QL 20%, we further observe the same bands at two different photon energies, providing a check that the gapped surface state is not an artifact of low photoemission cross section at a special photon energy. Our results on 4QL/1QL 10%, 4QL/1QL 15%, and 3QL/3QL 20% provide a systematic check of our results.

DISCUSSION

Our ARPES spectra show that we have realized the first emergent band structure in a lattice of topological interface states. We further demonstrate that we can tune this band structure through a topological phase transition. We summarize our results by plotting the compositions of Fig. 2 on a phase diagram as a function of t'/t (Fig. 5A). Our results can also be understood in terms of a one-dimensional atomic chain terminated either on a strong or on a weak bond. It is natural to ask whether any rigorous analogy exists between our topological insulator heterostructure and a one-dimensional topological phase (*22*). An interesting property of our heterostructure is that it naturally gives rise to an approximate chiral symmetry along the stacking direction. In particular, because

the wave function of a topological insulator surface state decays rapidly into the bulk, we expect that the only relevant hybridization in our heterostructure takes place between adjacent interface states. Further, along the stacking direction, the lattice is bipartite. The nearest-neighbor hopping on a bipartite lattice gives rise to an emergent chiral symmetry along the stacking direction. We note that chiral symmetry is required for a number of topological phases in one dimension, including the BDI, CII, DIII, and CI classes, as well as the well-known Su-Schrieffer-Heeger model (*20*–*22*). We suggest that future theoretical work could determine whether a one-dimensional topological phase might be realized in our system. Specifically, we might consider topological invariants on the one-dimensional band structure along k_z at fixed $k_{\|} = 0$. We also note that we may introduce a second nearest-neighbor hopping by using even thinner layers (see Fig. 5B). This may break the chiral symmetry, removing the one-dimensional topological invariant and shifting the surface state out of the superlattice bulk band gap. This would provide a direct experimental signature of the one-dimensional topological invariant. Another application of our topological insulator heterostructure is to break inversion symmetry using a unit cell consisting of four layers of different thicknesses (see Fig. 5C). This may lead to a superlattice band structure of spinful bands. More complicated topological insulator heterostructures may allow us to engineer time-reversal broken one-dimensional topological phases or large degeneracies implemented by fine-tuning hopping amplitudes. Our systematic ARPES measurements demonstrate the first atomic chain of topological insulator surface states. In this way, we provide not only an entirely novel type of condensed matter lattice but also a new platform to engineer band structures in true electron systems by directly controlling how electrons hop between lattice sites.

MATERIALS AND METHODS

Heterostructure growth

High-quality $Bi_2Se_3/In_xBi_{2-x}Se_3$ heterostructures were grown on 10 mm × 10 mm × 0.5 mm Al_2O_3 (0001) substrates using a custom-built SVTA MOS-V-2 molecular beam epitaxy system with a base pressure of 2×10^{-10} torr. Substrates were cleaned ex situ by 5-min exposure to ultraviolet-generated ozone and in situ by heating them to 800°C at an oxygen pressure of 1×10^{-6} torr for 10 min. Elemental Bi, In, and Se sources (99.999% pure) were thermally evaporated using effusion cells equipped with individual shutters. In all samples, the first layer of the superlattice was Bi_2Se_3, 3QL of which was grown at 135°C and annealed to 265°C for the rest of the film growth (*23*). For $In_xBi_{2-x}Se_3$ growth, Bi and In were coevaporated by simultaneously opening both shutters, whereas the Se shutter was kept open at all times during the growth. To accurately determine the concentration of In in the $In_xBi_{2-x}Se_3$ layers, source fluxes were calibrated in situ by a quartz crystal microbalance and ex situ by Rutherford backscattering, which, together, provide a measure of the In concentration accurate to within ~1%. All heterostructures had a total thickness of 59QL or 60QL, depending on the unit cell. In this way, all heterostructures consisted of ~ 10 unit cells. All samples were capped at room temperature in situ by an approximately 100-nm-thick protective Se layer to prevent surface contamination in atmosphere. Before capping by Se, the high quality of the heterostructure was checked by reflective high-energy electron diffraction (see fig. S1).

ARPES measurements

ARPES measurements were carried out at several synchrotron light sources, in particular at ANTARES, Synchrotron SOLEIL (Saint-Aubin, France); ADRESS, Swiss Light Source (Villigen, Switzerland); the HRPES end station of Surface and Interface Spectroscopy, Swiss Light Source; I05, Diamond Light Source (Oxfordshire, U.K.); and CASSIOPEE, SOLEIL. Samples were clamped onto the sample holder using either an Mo or Ta clamp screwed onto the sample base or thin strips of Ta foil spot-welded onto the sample base. In addition to securely mounting the sample, the clamp also provided electrical grounding. The Se capping layer was removed by heating the sample in a vacuum preparation chamber at temperatures between 200° and 300°C and at pressures lower than 10^{-9} torr, for ~ 1 hour. Following decapping, the quality of the exposed sample surface was checked by low-energy electron diffraction at a typical electron beam energy of 100 V. The presence of sharp Bragg peaks and their sixfold rotation symmetry (Fig. 1H) shows the high quality of the exposed sample surface. ARPES measurements were carried out at pressures lower than 10^{-10} torr at incident photon energies between 15 and 320 eV. We take a short Fermi surface mapping near the center of the Brillouin zone for each sample, at relevant photon energies, to identify the rotation angles corresponding to $\bar{\Gamma}$. This allows us to take ε-k cuts through the $\bar{\Gamma}$ point to within a rotation angle of ±0.15°, minimizing the error in our measurement of the band gap due to sample misalignment.

SUPPLEMENTARY MATERIALS

Supplementary material for this article is available at http://advances.sciencemag.org/cgi/content/full/3/3/e1501692/DC1

Estimate of indium diffusion in the heterostructure
Observation of a topological phase transition in numerics
Fine dependence on indium doping
Comparison with a single thin film of Bi_2Se_3
Detailed analysis of bulk quantum well states
fig. S1. Characterization of In diffusion in the heterostructures.
fig. S2. Topological phase transition in numerics.
fig. S3. Change in Fermi level with In doping.
fig. S4. Dimerized-limit heterostructure and a single thin film of Bi_2Se_3.
fig. S5. Bulk quantum well states of 4QL/2QL 15% and 4QL/1QL 20%.
Reference (*25*)

REFERENCES AND NOTES

1. G. Jotzu, M. Messer, R. Desbuquois, M. Lebrat, T. Uehlinger, D. Greif, T. Esslinger, Experimental realization of the topological Haldane model with ultracold fermions. *Nature* **515**, 237–240 (2014).
2. L. Lu, Z. Wang, D. Ye, L. Ran, L. Fu, J. D. Joannopoulos, M. Soljačić, Experimental observation of Weyl points. *Science* **349**, 622–624 (2015).
3. E. J. Mele, The winding road to topological insulators. *Phys. Scr.* **2015**, 014004 (2015).
4. M. Z. Hasan, C. L. Kane, *Colloquium*: Topological insulators. *Rev. Mod. Phys.* **82**, 3045–3067 (2010).
5. A. Burkov, L. Balents, Weyl semimetal in a topological insulator multilayer. *Phys. Rev. Lett.* **107**, 127205 (2011).
6. M. Brahlek, N. Koirala, J. Liu, T. I. Yusufaly, M. Salehi, M.-G. Han, Y. Zhu, D. Vanderbilt, S. Oh, Tunable inverse topological heterostructure utilizing $(Bi_{1-x}In_x)_2Se_3$ and multichannel weak-antilocalization effect. *Phys. Rev. B* **93**, 125416 (2016).
7. Z. Y. Wang, X. Guo, H. D. Li, T. L. Wong, N. Wang, M. H. Xie, Superlattices of Bi_2Se_3/In_2Se_3: Growth characteristics and structural properties. *Appl. Phys. Lett.* **99**, 023112 (2011).
8. Y. Zhao, H. Liu, X. Guo, Y. Jiang, Y. Sun, H. Wang, Y. Wang, H.-D. Li, M.-H. Xie, X.-C. Xie, J. Wang, Crossover from 3D to 2D quantum transport in Bi_2Se_3/In_2Se_3 superlattices. *Nano Lett.* **14**, 5244–5249 (2014).
9. Y. Xia, D. Qian, D. Hsieh, L. Wray, A. Pal, H. Lin, A. Bansil, D. Grauer, Y. S. Hor, R. J. Cava, M. Z. Hasan, Observation of a large-gap topological-insulator class with a single Dirac cone on the surface. *Nat. Phys.* **5**, 398–402 (2009).
10. H. J. Zhang, C.-X. Liu, X.-L. Qi, X. Dai, Z. Fang, S.-C. Zhang, Topological insulators in Bi_2Se_3, Bi_2Te_3 and Sb_2Te_3 with a single Dirac cone on the surface. *Nat. Phys.* **5**, 438–442 (2009).
11. M. Brahlek, N. Bansal, N. Koirala, S.-Y. Xu, M. Neupane, C. Liu, M. Z. Hasan, S. Oh, Topological-metal to band-insulator transition in $(Bi_{1-x}In_x)_2Se_3$ thin films. *Phys. Rev. Lett.* **109**, 186403 (2012).

12. X.-L. Qi, S.-C. Zhang, Topological insulators and superconductors. *Rev. Mod. Phys.* **83**, 1057–1110 (2011).
13. B. A. Bernevig, *Topological Insulators and Topological Superconductors* (Princeton Univ. Press, 2013).
14. M. Z. Hasan, J. E. Moore, Three-dimensional topological insulators. *Annu. Rev. Condens. Matter Phys.* **2**, 55–78 (2011).
15. M. Z. Hasan, S.-Y. Xu, G. Bian, Topological insulators, topological superconductors and Weyl fermion semimetals: Discoveries, perspectives and outlooks. *Phys. Scr.* **2015**, 014001 (2015).
16. M. Neupane, A. Richardella, J. Sánchez-Barriga, S.-Y. Xu, N. Alidoust, I. Belopolski, C. Liu, G. Bian, D. Zhang, D. Marchenko, A. Varykhalov, O. Rader, M. Leandersson, T. Balasubramanian, T.-R. Chang, H.-T. Jeng, S. Basak, H. Lin, A. Bansil, N. Samarth, M. Z. Hasan, Observation of quantum-tunneling modulated spin texture in ultrathin topological insulator Bi_2Se_3 films. *Nat. Commun.* **5**, 3841 (2014).
17. Y. Zhang, K. He, C.-Z. Chang, C.-L. Song, L.-L. Wang, X. Chen, J.-F. Jia, Z. Fang, X. Dai, W.-Y. Shan, S.-Q. Shen, Q. Niu, X.-L. Qi, S.-C. Zhang, X.-C. Ma, Q.-K. Xue, Crossover of the three-dimensional topological insulator Bi_2Se_3 to the two-dimensional limit. *Nat. Phys.* **6**, 584–588 (2010).
18. P. Yu, M. Cardona, *Fundamentals of Semiconductors* (Springer, 2001), chap. 9.
19. L. Esaki, R. Tsu, Superlattice and negative differential conductivity in semiconductors. *IBM J. Res. Dev.* **14**, 61–65 (1970).
20. W. P. Su, J. R. Schrieffer, A. J. Heeger, Solitons in polyacetylene. *Phys. Rev. Lett.* **42**, 1698–1701 (1979).
21. A. J. Heeger, S. Kivelson, J. R. Schrieffer, W.-P. Su, Solitons in conducting polymers. *Rev. Mod. Phys.* **60**, 781–850 (1988).
22. A. P. Schnyder, S. Ryu, A. Furusaki, A. W. W. Ludwig, Classification of topological insulators and superconductors in three spatial dimensions. *Phys. Rev. B* **78**, 195125 (2008).
23. N. Bansal, Y. S. Kim, E. Edrey, M. Brahlek, Y. Horibe, K. Iida, M. Tanimura, G.-H. Li, T. Feng, H.-D. Lee, T. Gustafsson, E. Andrei, S. Oh, Epitaxial growth of topological insulator Bi_2Se_3 film on Si(111) with atomically sharp interface. *Thin Solid Films* **520**, 224–229 (2011).
24. V. N. Strocov, X. Wang, M. Shi, M. Kobayashi, J. Krempasky, C. Hess, T. Schmitt, L. Patthey, Soft-x-ray ARPES facility at the ADRESS beamline of the SLS: Concepts, technical realisation and scientific applications. *J. Synchrotron Radiat.* **21**, 32–44 (2014).
25. N. Koirala, M. Brahlek, M. Salehi, L. Wu, J. Da, J. Waugh, T. Nummy, M.-G. Han, J. Moon, Y. Zhu, D. Dessau, W. Wu, N. P. Armitage, S. Oh, Record surface state mobility and quantum hall effect in topological insulator thin films via interface engineering. *Nano Lett.* **15**, 8245–8249 (2015).

Acknowledgments

Funding: Work at Princeton University and synchrotron-based ARPES measurements led by Princeton University were supported by the U.S. Department of Energy under Basic Energy Sciences grant no. DE-FG-02-05ER46200 (to M.Z.H.). I.B. acknowledges the support of the NSF Graduate Research Fellowship Program. N.K., M.B., and S.O. were supported by the Emergent Phenomena in Quantum Systems Initiative of the Gordon and Betty Moore Foundation under grant no. GBMF4418 and by the NSF under grant no. NSF-EFMA-1542798. H.L. acknowledges support from the Singapore National Research Foundation under award no. NRF-NRFF2013-03. M.N. was supported by start-up funds from the University of Central Florida. We acknowledge Diamond Light Source, Didcot, U.K., for time on beamline I05 under proposal SI11742-1. We acknowledge measurements carried out at the ADRESS beamline (*24*) of the Swiss Light Source, Paul Scherrer Institute, Switzerland. We acknowledge J. D. Denlinger, S. K. Mo, and A. V. Fedorov for support at the Advanced Light Source, Lawrence Berkeley National Laboratory, Berkeley, CA, USA. C.L. was supported by grant no. 11504159 of the National Natural Science Foundation of China (NSFC), grant no. 2016A030313650 of NSFC Guangdong, and project no. JCY20150630145302240 of the Shenzhen Science and Technology Innovations Committee. **Author contributions:** I.B., S.-Y.X., and M.Z.H. conceived the study. N.K., M.B., and S.O. grew and characterized the heterostructures. N.K. and V.N.S. provided crucial creative insight into heterostructure growth and measurement. I.B. carried out synchrotron ARPES measurements with assistance from S.-Y.X., C.L., G.B., M.N., N.A., D.S., and H.Z. V.N.S., V.R., T.K., N.C.P., C.C., F.B., P.L.F., A.T.-I., M.-C.A., M.S., and M.H. built and supported the synchrotron ARPES end stations. G.C. and H.L. carried out numerical calculations. M.Z.H. provided overall direction, planning, and guidance for the project. **Competing interests:** The authors declare that they have no competing interests. **Data and materials availability:** All data needed to evaluate the conclusions in the paper are present in the paper and/or the Supplementary Materials. Additional data related to this paper may be requested from the authors.

Submitted 23 November 2015
Accepted 28 February 2017
Published 24 March 2017
10.1126/sciadv.1501692

Citation: I. Belopolski, S.-Y. Xu, N. Koirala, C. Liu, G. Bian, V. N. Strocov, G. Chang, M. Neupane, N. Alidoust, D. Sanchez, H. Zheng, M. Brahlek, V. Rogalev, T. Kim, N. C. Plumb, C. Chen, F. Bertran, P. Le Fèvre, A. Taleb-Ibrahimi, M.-C. Asensio, M. Shi, H. Lin, M. Hoesch, S. Oh, M. Z. Hasan, A novel artificial condensed matter lattice and a new platform for one-dimensional topological phases. *Sci. Adv.* **3**, e1501692 (2017).